Small-x Physics and EIC

Bo-Wen Xiao

School of Science and Engineering,
The Chinese University of Hong Kong, Shenzhen

2022 Summer School at Fudan University
August, 2022

References:

- Peskin and Schroeder, An Introduction to Quantum Field Theory.
- R.D. Field, Applications of perturbative QCD A lot of detailed examples.
- R. K. Ellis, W. J. Stirling and B. R. Webber, QCD and Collider Physics
- Y. Kovchegov and E. Levin, Quantum Chromodynamics at High Energy
- "Electron Ion Collider: The Next QCD Frontier: Understanding the glue that binds us all," Eur. Phys. J. A **52**, no.9, 268 (2016) [arXiv:1212.1701 [nucl-ex]].
- "Science Requirements and Detector Concepts for the Electron-Ion Collider: EIC Yellow Report," [arXiv:2103.05419 [physics.ins-det]].

Outline

1 QFT Basics and Theory Backgrounds
- Infrared Safe Observables
- Collinear and TMD Factorization

2 Introduction to Saturation Physics
- Weizsäcker-Williams Methods
- McLerran-Venugopalan Model
- Small-x evolution equations (BFKL + BK)

3 EIC Physics
- Overview
- Observables at EIC

Infrared Safety

- Two kinds of IR divergences: collinear and soft divergences.
  - According to uncertainty principle, soft $\leftrightarrow$ long distance;
  - Takes a long time to separate two collinear particles.
- For a suitable defined inclusive observable (e.g., $\sigma_{e^+e^-\to\text{hadrons}}$), there is a cancellation between the soft and collinear singularities occurring in the real and virtual contributions. Kinoshita-Lee-Nauenberg theorem
- Any new observables must have a definition which does not distinguish between

$$\text{parton} \leftrightarrow \text{parton + soft gluon}$$
$$\text{parton} \leftrightarrow \text{two collinear partons}$$

- Observables that respect the above constraint are called infrared safe observables. Infrared safety is a requirement that the observable is calculable in pQCD.
- Other infrared safe observables, for example, Thrust: $T = \max \frac{\sum_i |p_i \cdot n|}{\sum_i |p_i|}$ ...

e^+e^- annihilation

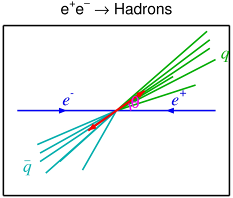

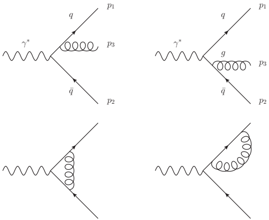

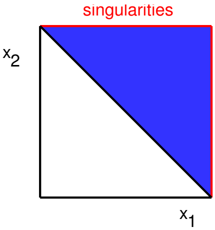

- Born diagram ( ) gives $\sigma_0 = \alpha_{em}\sqrt{s}N_c \sum_q e_q^2 \left(\frac{4\pi\mu^2}{s}\right)^{\epsilon} \frac{\Gamma[2-\epsilon]}{\Gamma[2-2\epsilon]}$
- NLO: real contribution (3 body final state). $x_i \equiv \frac{2E_i}{Q}$ with $Q = \sqrt{s}$

$$\frac{d\sigma_3}{dx_1 dx_2} = C_F \frac{\alpha_s}{2\pi}\sigma_0 \frac{x_1^2 + x_2^2}{(1-x_1)(1-x_2)}$$

e^+e^- annihilation

- NLO: real contribution (3 body final state). $x_i \equiv \frac{2E_i}{Q}$ with $Q = \sqrt{s}$

$$\frac{d\sigma_3}{dx_1 dx_2} = C_F \frac{\alpha_s}{2\pi}\sigma_0 \frac{x_1^2 + x_2^2}{(1-x_1)(1-x_2)}$$

$$\text{with} \quad \frac{1}{(1-x_1)(1-x_2)} = \frac{1}{x_3}\left[\frac{1}{(1-x_1)} + \frac{1}{(1-x_2)}\right]$$

- Energy conservation $\Rightarrow x_1 + x_2 + x_3 = 2$.
- $(p_1 + p_3)^2 = 2p_1 \cdot p_3 = (Q - p_2)^2 = Q^2(1 - x_2)$
- $x_2 \to 1 \Rightarrow \vec{p}_3 \,||\, \vec{p}_1 \Rightarrow$ Collinear Divergence (Similarly $x_1 \to 1$)
- $x_3 \to 0 \Rightarrow$ Soft Divergence.

Dimensional Regularization

Dimensional regularization:

- Analytically continue in the number of dimensions from $d = 4$ to $d = 4 - 2\epsilon$.
- Convert the soft and collinear divergence into poles in ϵ.
- To keep g_s dimensionless, substitue $g_s \to g_s \mu^\epsilon$ with renormalization scale μ.

At the end of the day, one finds

$$\sigma_r = \sigma_0 \frac{\alpha_s(\mu)}{2\pi} C_F \left(\frac{Q^2}{4\pi\mu^2}\right)^{-\epsilon} \frac{\Gamma[1-\epsilon]}{\Gamma[1-2\epsilon]} \left[\frac{2}{\epsilon^2} + \frac{3}{\epsilon} + \frac{19}{2} - \frac{2\pi^2}{3}\right]$$

$$\sigma_v = \sigma_0 \frac{\alpha_s(\mu)}{2\pi} C_F \left(\frac{Q^2}{4\pi\mu^2}\right)^{-\epsilon} \frac{\Gamma[1-\epsilon]}{\Gamma[1-2\epsilon]} \left[-\frac{2}{\epsilon^2} - \frac{3}{\epsilon} - 8 + \frac{2\pi^2}{3}\right]$$

and the sum $\lim_{\epsilon\to 0} \sigma = \sigma_0 \left(1 + \frac{3}{4} C_F \frac{\alpha_s(\mu)}{\pi} + \mathcal{O}(\alpha_s^2)\right)$.

- (Almost) Complete Cancellation between real and virtual.
- For more exclusive observables, the cancellation is not always complete.

Thrust

Global observable reflecting the structure of the hadronic events in e^+e^-:

$$T = \max_{\vec{n}} \frac{\sum_i |p_i \cdot n|}{\sum_i |p_i|}$$

$T = 1$

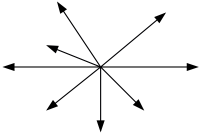

$T = 1/2$

Thrust

- For 3-particle events, in terms of x_1 and x_2, the cross section is

$$\frac{d\sigma_3}{\sigma_0 dx_1 dx_2} = \frac{C_F \alpha_s}{2\pi} \frac{x_1^2 + x_2^2}{(1-x_1)(1-x_2)}$$

- For 3-particle events, $T = \max[x_1, x_2, x_3]$
- By symmetrizing x_i, and requiring $x_1 > x_2 > x_3$, we get $T = x_1 > 2/3$ and

$$\begin{aligned} \frac{d\sigma_3}{\sigma_0 dT} &= \frac{2C_F\alpha_s}{2\pi} \int_{1-2T}^{T} \mathrm{d}x_2 \left[\frac{x_1^2 + x_2^2}{(1-x_1)(1-x_2)} + (x_1 \to x_3) + (x_2 \to x_3) \right] \\ &= \frac{C_F\alpha_s}{2\pi} \left[\frac{2(3T^2 - 3T + 2)}{T(1-T)} \ln \frac{2T-1}{1-T} - \frac{3(3T-2)(2-T)}{1-T} \right] \end{aligned}$$

Thrust

$$\frac{d\sigma_3}{\sigma_0 dT} = \frac{C_F\alpha_s}{2\pi}\left[\frac{2(3T^2-3T+2)}{T(1-T)}\ln\frac{2T-1}{1-T}+\frac{3(2-3T)(2-T)}{1-T}\right]$$

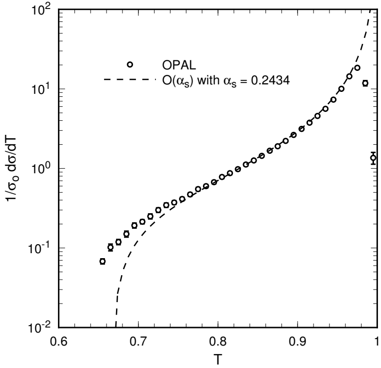

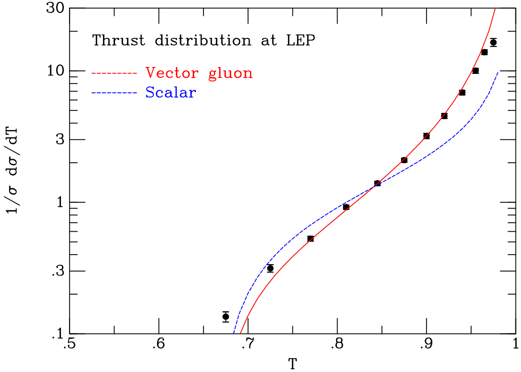

Thrust

- Deficiency at low T due to kinematics. $T > 2/3$ at this order.
- Miss the data when $T \to 1$ due to divergence. Sudakov factor!

$$\frac{d\sigma}{\sigma_0 dT}\Big|_{T\to 1} \sim \frac{4C_F\alpha_s}{2\pi}\frac{4}{(1-T)}\ln\frac{1}{1-T}\exp\left[-\frac{\alpha_s C_F}{\pi}\ln^2(1-T)\right]$$

- Indication of gluon being a vector boson instead of a scalar.

Outline

1 QFT Basics and Theory Backgrounds
- Infrared Safe Observables
- Collinear and TMD Factorization

2 Introduction to Saturation Physics
- Weizsäcker-Williams Methods
- McLerran-Venugopalan Model
- Small-x evolution equations (BFKL + BK)

3 EIC Physics
- Overview
- Observables at EIC

Light Cone coordinates and gauge

For a relativistic hadron moving in the $+z$ direction

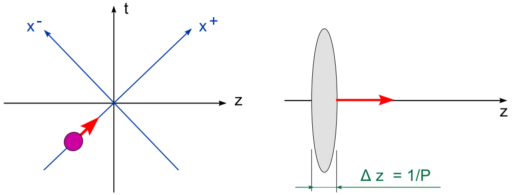

- In this frame, the momenta are defined

$$P^+ = \frac{1}{\sqrt{2}}(P^0 + P^3) \quad \text{and} \quad P^- = \frac{1}{\sqrt{2}}(P^0 - P^3) \to 0; \qquad P^2 = 2P^+P^- - P_\perp^2$$

- Light cone gauge for a gluon with $k^\mu = (k^+, k^-, k_\perp)$, polarization vector

$$k^\mu \epsilon_\mu = 0 \Rightarrow \quad \epsilon = (\epsilon^+ = 0, \epsilon^- = \frac{\epsilon_\perp \cdot k_\perp}{k^+}, \epsilon_\perp^\pm) \quad \text{with} \quad \epsilon_\perp^\pm = \frac{1}{\sqrt{2}}(1, \pm i)$$

Deep inelastic scattering (DIS)

Kinematics of Lepton-Nucleon Scattering

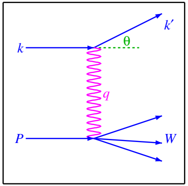

$$\frac{\mathrm{d}\sigma}{\mathrm{d}E'\mathrm{d}\Omega} = \frac{\alpha_{\mathrm{em}^2}}{Q^4}\frac{E'}{E} L_{\mu\nu} W^{\mu\nu}$$

with $L_{\mu\nu}$ the leptonic tensor and $W^{\mu\nu}$ defined as

$$W^{\mu\nu} = \left(-g^{\mu\nu} + \frac{q_\mu q_\nu}{q^2}\right) W_1 + \frac{1}{m_p^2}\left(P^\mu - \frac{P\cdot q}{q^2} q^\mu\right)\left(P^\nu - \frac{P\cdot q}{q^2} q^\nu\right) W_2$$

Introduce the dimensionless structure function:

$$F_1 \equiv W_1 \quad \text{and} \quad F_2 \equiv \frac{Q^2}{2m_p x} W_2$$

$$\Rightarrow \frac{\mathrm{d}\sigma}{\mathrm{d}x\mathrm{d}y} = \frac{\alpha_{4\pi s \mathrm{em}^2}}{Q^4}\left[(1-y)F_2 + xy^2 F_1\right] \quad \text{with} \quad y = \frac{P\cdot q}{P\cdot k}.$$

Callan-Gross relation

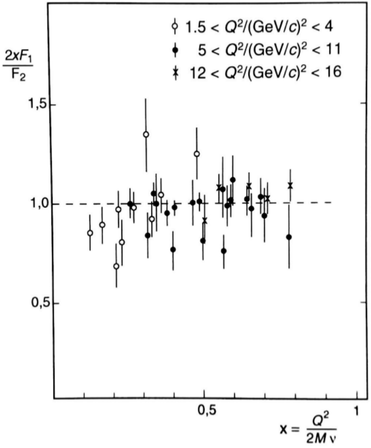

- Quark Parton Model: Callan-Gross relation

$$F_2(x) = 2xF_1(x) = \sum_q e_q^2 x \left[f_q(x) + f_{\bar{q}}(x)\right].$$

- The above relation ($F_2 = 2xF_1$) follows from the fact that a spin-$\frac{1}{2}$ quark cannot absorb a longitudinally polarized vector boson.
- In contrast, spin-0 quark cannot absorb transverse bosons, and thus it would give $F_1 = 0$.

Parton Density

The probabilistic interpretation of the parton density.

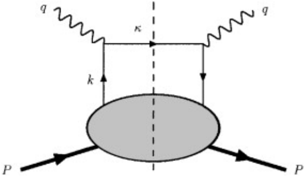

$$\Rightarrow \quad f_q(x) = \int \frac{\mathrm{d}\zeta^-}{4\pi} e^{ixP^+\zeta^-} \langle P \left| \bar{\psi}(0)\gamma^+\psi(0,\zeta^-) \right| P \rangle$$

Comments:

- Gauge link $\mathcal{L}$ is necessary to make the parton density gauge invariant.

$$\mathcal{L}(0,\zeta^-) = \mathcal{P} \exp\left(\int_0^{\zeta^-} \mathrm{d}s_\mu A^\mu \right)$$

- Choose light cone gauge $A^+ = 0$ and B.C., one can eliminate the gauge link.
- Now we can interpret $f_q(x)$ as parton density in the light cone frame.

Drell-Yan process

For lepton pair productions in hadron-hadron collisions:

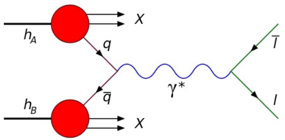

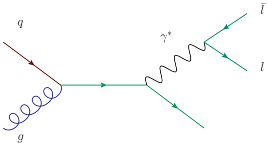

the cross section is

$$\frac{\mathrm{d}\sigma}{\mathrm{d}M^2\mathrm{d}Y} = \sum_q x_1 f_q(x_1) x_2 f_{\bar{q}}(x_2) \frac{1}{3} e_q^2 \frac{4\pi\alpha^2}{3M^4} \quad \text{with} \quad Y = \frac{1}{2} \ln \frac{x_1}{x_2}.$$

- Collinear factorization: $f_q(x)$ involved in DIS and Drell-Yan process are the same.
- At low-x and high energy, the dominant channel is $qg \to q\gamma^*(l^+l^-)$.

Fragmentation function

Factorization of single inclusive hadron production in e^+e^-:

$$\frac{1}{\sigma_0}\frac{\mathrm{d}\sigma(e^+e^- \to h+X)}{\mathrm{d}x} = \sum_i \int_x^1 C_i\left(z, \alpha_s(\mu^2), s/\mu^2\right) D_{h/i}(x/z, \mu^2) + \mathcal{O}(1/s)$$

- $D_{h/i}(x/z, \mu^2)$ encodes the probability that the parton i fragments into a hadron h carrying a fraction z of the parton's momentum.
- Energy conservation $\Rightarrow$

$$\sum_h \int_0^1 dzzD_i^h(z, \mu^2) = 1$$

- Heavy quark fragmentation function: Peterson fragmentation function

Evolution of parton density: Change of resolution

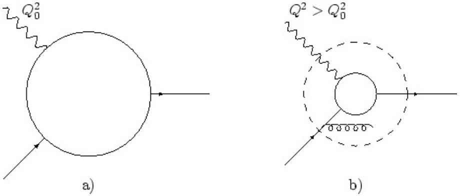

Large x: valence quarks

Small x: Gluons, sea quarks

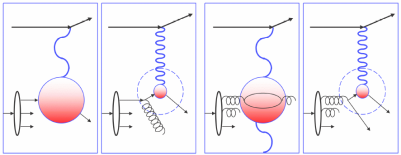

DGLAP Splitting function

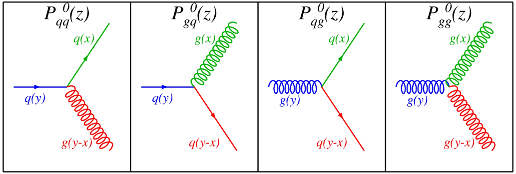

$$\xi = z = \frac{x}{y}$$

$$\mathcal{P}^0_{qq}(\xi) = \frac{1+\xi^2}{(1-\xi)_+} + \frac{3}{2}\delta(1-\xi);\ \mathcal{P}^0_{gq}(\xi) = \frac{1}{\xi}\left[1+(1-\xi)^2\right];\ \mathcal{P}^0_{qg}(\xi) = \left[(1-\xi)^2+\xi^2\right];$$

$$\mathcal{P}^0_{gg}(\xi) = 2\left[\frac{\xi}{(1-\xi)_+} + \frac{1-\xi}{\xi} + \xi(1-\xi)\right] + \left(\frac{11}{6} - \frac{2N_f T_R}{3N_c}\right)\delta(1-\xi).$$

- $\int_0^1 \frac{d\xi f(\xi)}{(1-\xi)_+} = \int_0^1 \frac{d\xi[f(\xi)-f(1)]}{1-\xi} \Rightarrow \int_0^1 \frac{d\xi}{(1-\xi)_+} = 0$

Derivation of $\mathcal{P}^0_{qq}(\xi)$

The real contribution:

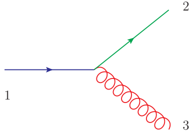

$$k_1 = (P^+, 0, 0_\perp) \quad ; \quad k_2 = (\xi P^+, \frac{k_\perp^2}{\xi P^+}, k_\perp)$$

$$k_3 = ((1-\xi)P^+, \frac{k_\perp^2}{(1-\xi)P^+}, -k_\perp) \quad \epsilon_3 = (0, -\frac{2k_\perp \cdot \epsilon_\perp^{(3)}}{(1-\xi)P^+}, \epsilon_\perp^{(3)})$$

$$|V_{q\to qg}|^2 = \frac{1}{2}\mathrm{Tr}\left(\not{k}_2\gamma_\mu \not{k}_1\gamma_\nu\right)\sum \epsilon_3^{*\mu}\epsilon_3^\nu = \frac{2k_\perp^2}{\xi(1-\xi)}\frac{1+\xi^2}{1-\xi}$$

$$\Rightarrow \mathcal{P}_{qq}(\xi) = \frac{1+\xi^2}{1-\xi} \quad (\xi < 1)$$

Derivation of $\mathcal{P}^0_{qq}(\xi)$

- Including the virtual graph 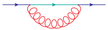, use $\int_a^1 \frac{\mathrm{d}\xi g(\xi)}{(1-\xi)_+} = \int_a^1 \frac{\mathrm{d}\xi g(\xi)}{1-\xi} - g(1)\int_0^1 \frac{\mathrm{d}\xi}{1-\xi}$

$$
\begin{aligned}
& \frac{\alpha_s C_F}{2\pi}\left[\int_x^1 \frac{\mathrm{d}\xi}{\xi} q(x/\xi)\frac{1+\xi^2}{1-\xi} - q(x)\int_0^1 \mathrm{d}\xi \frac{1+\xi^2}{1-\xi}\right] \\
= \quad & \frac{\alpha_s C_F}{2\pi}\left[\int_x^1 \frac{\mathrm{d}\xi}{\xi} q(x/\xi)\frac{1+\xi^2}{(1-\xi)_+} - q(x)\underbrace{\int_0^1 \mathrm{d}\xi \frac{1+\xi^2}{(1-\xi)_+}\right]}_{=-\frac{3}{2}}.
\end{aligned}
$$

- Common practice in calculating the virtual graphs. (Also see HW.)

Derivation of $\mathcal{P}^0_{qq}(\xi)$

- Regularize $\frac{1}{1-\xi}$ to $\frac{1}{(1-\xi)_+}$ by including the divergence from the virtual graph.
- Probability conservation:

$$P_{qq} + \mathrm{d}P_{qq} = \delta(1-\xi) + \frac{\alpha_s C_F}{2\pi}\mathcal{P}^0_{qq}(\xi)dt \quad \text{and} \quad \int_0^1 \mathrm{d}\xi \mathcal{P}_{qq}(\xi) = 0,$$

$$\Rightarrow \mathcal{P}_{qq}(\xi) = \frac{1+\xi^2}{(1-\xi)_+} + \frac{3}{2}\delta(1-\xi) = \left(\frac{1+\xi^2}{1-\xi}\right)_+ .$$

Derivation of $\mathcal{P}_{gg}^{0}(\xi)$

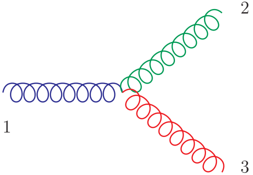

$$k_1 = (P^+, 0, 0_\perp) \quad \epsilon_1 = (0, 0, \epsilon_\perp^{(1)}) \quad \text{with} \quad \epsilon_\perp^{\pm} = \frac{1}{\sqrt{2}}(1, \pm i)$$

$$k_2 = (\xi P^+, \frac{k_\perp^2}{\xi P^+}, k_\perp) \quad \epsilon_2 = (0, \frac{2k_\perp \cdot \epsilon_\perp^{(2)}}{\xi P^+}, \epsilon_\perp^{(2)})$$

$$k_3 = ((1-\xi)P^+, \frac{k_\perp^2}{(1-\xi)P^+}, -k_\perp) \quad \epsilon_3 = (0, -\frac{2k_\perp \cdot \epsilon_\perp^{(3)}}{(1-\xi)P^+}, \epsilon_\perp^{(3)})$$

$$V_{g\to gg} = (k_1 + k_3) \cdot \epsilon_2 \epsilon_1 \cdot \epsilon_3 + (k_2 - k_3) \cdot \epsilon_1 \epsilon_2 \cdot \epsilon_3 - (k_1 + k_2) \cdot \epsilon_3 \epsilon_1 \cdot \epsilon_2$$

$$\Rightarrow \quad |V_{g\to gg}|^2 = |V_{+++}|^2 + |V_{+-+}|^2 + |V_{++-}|^2 = 4k_\perp^2 \frac{[1-\xi(1-\xi)]^2}{\xi^2(1-\xi)^2}$$

$$\Rightarrow \quad \mathcal{P}_{gg}(\xi) = 2\left[\frac{1-\xi}{\xi} + \frac{\xi}{1-\xi} + \xi(1-\xi)\right] \quad (\xi < 1)$$

Derivation of $\mathcal{P}^0_{gg}(\xi)$

$$V_{g\to gg} = (k_1 + k_3)\cdot\epsilon_2\epsilon_1\cdot\epsilon_3 + (k_2 - k_3)\cdot\epsilon_1\epsilon_2\cdot\epsilon_3 - (k_1 + k_2)\cdot\epsilon_3\epsilon_1\cdot\epsilon_2$$

$$\Rightarrow \quad |V_{g\to gg}|^2 = |V_{+++}|^2 + |V_{+-+}|^2 + |V_{++-}|^2 = 4k_\perp^2 \frac{[1-\xi(1-\xi)]^2}{\xi^2(1-\xi)^2}$$

$$\Rightarrow \quad \mathcal{P}_{gg}(\xi) = 2\left[\frac{1-\xi}{\xi} + \frac{\xi}{1-\xi} + \xi(1-\xi)\right] \quad (\xi < 1)$$

- Regularize $\frac{1}{1-\xi}$ to $\frac{1}{(1-\xi)_+}$
- Momentum conservation:

$$\int_0^1 \mathrm{d}\xi\,\xi\,[\mathcal{P}_{qq}(\xi) + \mathcal{P}_{gq}(\xi)] = 0 \quad \int_0^1 \mathrm{d}\xi\,\xi\,[2\mathcal{P}_{qg}(\xi) + \mathcal{P}_{gg}(\xi)] = 0,$$

$\Rightarrow$ the terms which is proportional to $\delta(1-\xi)$.

DGLAP equation

In the leading logarithmic approximation with $t = \ln \mu^2$, the parton distribution and fragmentation functions follow the DGLAP[Dokshitzer, Gribov, Lipatov, Altarelli, Parisi, 1972-1977] evolution equation as follows:

$$\frac{\mathrm{d}}{\mathrm{d}t}\begin{bmatrix} q(x,\mu) \\ g(x,\mu) \end{bmatrix} = \frac{\alpha(\mu)}{2\pi}\int_x^1 \frac{d\xi}{\xi}\begin{bmatrix} C_F P_{qq}(\xi) & T_R P_{qg}(\xi) \\ C_F P_{gq}(\xi) & N_c P_{gg}(\xi) \end{bmatrix}\begin{bmatrix} q(x/\xi,\mu) \\ g(x/\xi,\mu) \end{bmatrix},$$

and

$$\frac{\mathrm{d}}{\mathrm{d}t}\begin{bmatrix} D_{h/q}(z,\mu) \\ D_{h/g}(z,\mu) \end{bmatrix} = \frac{\alpha(\mu)}{2\pi}\int_z^1 \frac{d\xi}{\xi}\begin{bmatrix} C_F P_{qq}(\xi) & C_F P_{gq}(\xi) \\ T_R P_{qg}(\xi) & N_c P_{gg}(\xi) \end{bmatrix}\begin{bmatrix} D_{h/q}(z/\xi,\mu) \\ D_{h/g}(z/\xi,\mu) \end{bmatrix},$$

Collinear Factorization at NLO

$\overline{\text{MS}}$ scheme ($\frac{1}{\hat{\epsilon}} = \frac{1}{\epsilon} + \ln 4\pi - \gamma_E$), DGLAP equation reads

$$\begin{bmatrix} q(x,\mu) \\ g(x,\mu) \end{bmatrix} = \begin{bmatrix} q^{(0)}(x) \\ g^{(0)}(x) \end{bmatrix} - \frac{1}{\hat{\epsilon}} \frac{\alpha(\mu)}{2\pi} \int_x^1 \frac{d\xi}{\xi} \begin{bmatrix} C_F P_{qq}(\xi) & T_R P_{qg}(\xi) \\ C_F P_{gq}(\xi) & N_c P_{gg}(\xi) \end{bmatrix} \begin{bmatrix} q(x/\xi) \\ g(x/\xi) \end{bmatrix},$$

$$\begin{bmatrix} D_{h/q}(z,\mu) \\ D_{h/g}(z,\mu) \end{bmatrix} = \begin{bmatrix} D^{(0)}_{h/q}(z) \\ D^{(0)}_{h/g}(z) \end{bmatrix} - \frac{1}{\hat{\epsilon}} \frac{\alpha(\mu)}{2\pi} \int_z^1 \frac{d\xi}{\xi} \begin{bmatrix} C_F P_{qq}(\xi) & C_F P_{gq}(\xi) \\ T_R P_{qg}(\xi) & N_c P_{gg}(\xi) \end{bmatrix} \begin{bmatrix} D_{h/q}(z/\xi) \\ D_{h/g}(z/\xi) \end{bmatrix}.$$

Factorization

One-loop factorization:

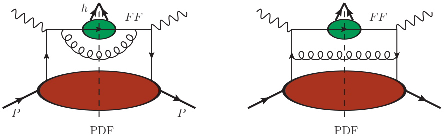

For gluon with momentum k

- Soft (k) divergence cancels between real and virtual diagrams;
- k is collinear to initial quark $\Rightarrow$ parton distribution function;
- k is collinear to the final state quark $\Rightarrow$ fragmentation function.
- KLN theorem does not apply to PDFs and FFs.
- Other kinematical region $\Rightarrow$ the NLO ($\mathcal{O}(\alpha_s)$ correction) hard factor.

Collinear Factorization vs $k_\perp$ Factorization

Collinear Factorization (Treat partons given by the integrated PDFs as having $k_\perp = 0$)

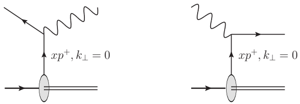

$k_\perp$ Factorization(Spin physics and saturation physics)

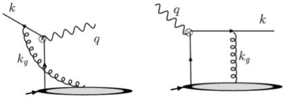

- The incoming partons carry no $k_\perp$ in the Collinear Factorization. (Approximation)
- In general, there is intrinsic $k_\perp$, which is sometimes not negligible.
- $k_\perp$ Factorization: High energy evolution with $k_\perp$ fixed.

DGLAP evolution

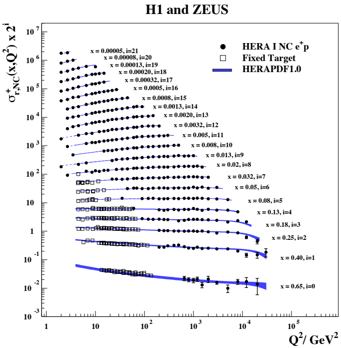

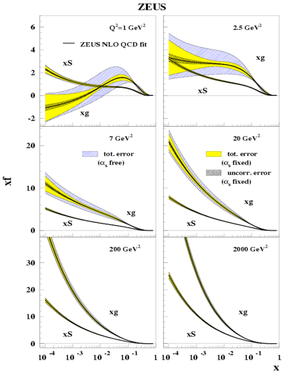

- NLO DGLAP fit yields negative gluon distribution at low Q^2 and low x.
- Does this mean there is no gluons in that region? No

Phase diagram in QCD

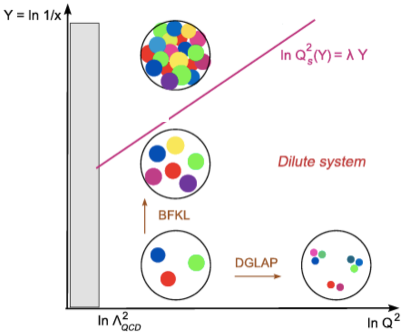

- Low Q^2 and low x region $\Rightarrow$ saturation region. (Use BFKL and BK equations instead)
- BK equation is the non-linear equation which describes the saturation physics.

k_t dependent parton distributions

The unintegrated quark distribution

$$f_q(x,k_\perp) = \int \frac{d\xi^- d^2\xi_\perp}{4\pi(2\pi)^2} e^{ixP^+\xi^- + i\xi_\perp\cdot k_\perp} \langle P \left| \bar{\psi}(0)\mathcal{L}^\dagger(0)\gamma^+\mathcal{L}(\xi^-,\xi_\perp)\psi(\xi_\perp,\xi^-) \right| P\rangle$$

cf. the itegrated PDF $\quad f_q(x) = \int \frac{d\xi^-}{4\pi} e^{ixP^+\xi^-} \langle P \left| \bar{\psi}(0)\gamma^+\mathcal{L}(\xi^-)\psi(0,\xi^-) \right| P\rangle$

- Gauge invariant def: The dependence of $\xi_\perp$ in the definition.
- Light-cone gauge + proper boundary condition $\Rightarrow$ parton density interpretation.
- The gauge links come from the resummation of multiple gluon interactions.
- Gauge links may vary among different processes.

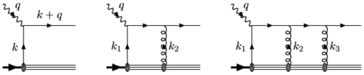

(a) (b) (c)

Outline

1 QFT Basics and Theory Backgrounds
- Infrared Safe Observables
- Collinear and TMD Factorization

2 Introduction to Saturation Physics
- Weizsäcker-Williams Methods
- McLerran-Venugopalan Model
- Small-x evolution equations (BFKL + BK)

3 EIC Physics
- Overview
- Observables at EIC

Weizsäcker-Williams Method of virtual quanta



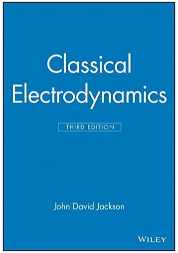

- Following Fermi[24], Weizsäcker [34] and Williams [35] discovered that the EM fields of a fast moving charged particle are almost transverse. (Equivalent Photon Approximation)
- A charged particle carries a cloud of quasi-real photons ready to be radiated if perturbed.
- Application in QCD: WW gluon distribution. [McLerran, Venugopalan, 94; Kovchegov, 96; Jalilian-Marian, Kovner, McLerran and Weigert, 97]
- Application in Gravitational Wave. [Aichelburg and Sexl, 71; Dray and 't Hooft, 85]

EPA and Weizsäcker-Williams Photon Distribution

Boost static potential to infinite momentum frame [Jackiw, Kabat and Ortiz, 92] and HW

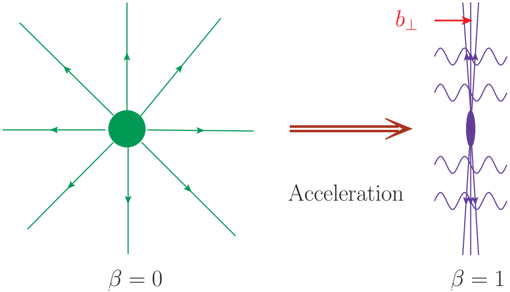

Static E fields $\Rightarrow$ Electro-Magnetic Wave

EPA and Weizsäcker-Williams Photon Distribution

Boost static potential to infinite momentum frame [Jackiw, Kabat and Ortiz, 92] and HW

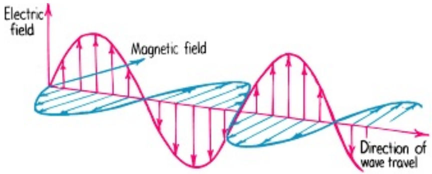

$$A^{+}_{Cov} = -\frac{q}{\pi}\ln(\lambda b_\perp)\delta(t-z),$$

$$\vec{E} = \frac{q}{2\pi}\frac{\vec{b}_\perp}{b_\perp^2}\delta(t-z),$$

$$\vec{B} = \frac{q}{2\pi}\frac{\hat{v}\times\vec{b}_\perp}{b_\perp^2}\delta(t-z),$$

$$\vec{A}^{LC}_{\perp} = -\frac{q}{2\pi}[\vec{\nabla}_\perp \ln(\lambda b_\perp)]\theta(t-z).$$

Static E fields $\Rightarrow$ Electro-Magnetic Wave

$\Rightarrow$ EM pulses are equivalent to a lot of photons

- The gauge potentials A_μ in Covariant gauge and LC gauge are related by a gauge transformation. λ is an irrelevant parameter setting the scale.
- Classical EM: transverse EM fields $\Leftrightarrow$ QM: Co-moving Quasi-real photons.

EPA and Weizsäcker-Williams Photon Distribution

- Classical EM: transverse EM fields ⇔ QM: Co-moving Quasi-real photons.

$$\text{CoV gauge} \qquad A^t_{Cov} = A^z_{Cov} = -\frac{q}{2\pi}\ln(\lambda b_\perp)\delta(t-z),$$

$$\text{LC gauge} \qquad \vec{A}^{LC}_\perp = -\frac{q}{2\pi}[\vec{\nabla}_\perp \ln(\lambda b_\perp)]\theta(t-z).$$

- The photon distribution in the transverse momentum space of a point particle

$$xf_\gamma(x,\vec{k}_\perp) = \int \frac{d\xi^- d^2\xi_\perp}{(2\pi)^3} e^{-ixP^+\xi^- - ik_\perp\cdot\xi_\perp} \left\langle A \left| F^{+i}\left(\frac{\xi}{2}\right) F^{+i}\left(-\frac{\xi}{2}\right) \right| A \right\rangle$$

$$= \frac{Z^2\alpha}{\pi^2}\frac{1}{k_\perp^2} \quad \text{with} \quad q = Ze.$$

Transverse Momentum Dependent (TMD) Photon Distribution

The photon distribution (flux) for nuclei

$$xf_\gamma(x, k_\perp) = \frac{Z^2\alpha}{\pi^2} \frac{k_\perp^2}{\left(k_\perp^2 + x^2M^2\right)^2} F_A(k^2) F_A(k^2)$$

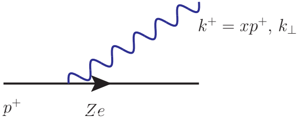

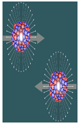

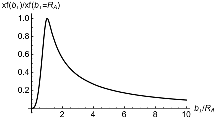

- $F_A(k^2)$ is the charge form factor with $k^2 = k_\perp^2 + x^2M^2$. $F_A = 1$ for point charge.
- Wood-Saxon or Gaussian models for realistic nuclei. (*Pb* is very bright!)
- Typical transverse momentum of the photon is $1/R_A$, which is 30MeV for *Pb*.

Linearly Polarized Photon

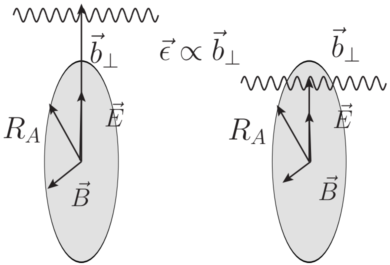

- E is linearly polarized along the impact parameter $b_\perp$ direction;
- $\vec{B} \perp \vec{E}$;
- The LC gauge potential $A_\perp \propto \vec{b}_\perp$;
- Polarization vector $\vec{\epsilon}_\perp = \vec{b}_\perp / b_\perp$.
- Similar case in momentum space.

Linearly Polarized Photon

- WW photon distribution is maximumly polarized, since $xf_\gamma = xh_\gamma$.

$$xf_\gamma^{ij}(x;b_\perp) = \int \frac{d^2\Delta_\perp}{(2\pi)^2} e^{i\Delta_\perp\cdot b_\perp} \langle A, -\frac{\Delta_\perp}{2}|F^{+i}F^{+j}|A, \frac{\Delta_\perp}{2}\rangle\ ,$$

$$xf_\gamma^{ij}(x;b_\perp) = \frac{\delta^{ij}}{2} xf_\gamma(x;b_\perp) + \left(\frac{b_\perp^i b_\perp^j}{b_\perp^2} - \frac{\delta^{ij}}{2}\right) xh_\gamma(x;b_\perp) = \frac{b_\perp^i b_\perp^j}{b_\perp^2} xf_\gamma,$$

$$xh_\gamma(x,b_\perp) = xf_\gamma(x,b_\perp) = 4Z^2\alpha \left| \int \frac{d^2k_\perp}{(2\pi)^2} e^{ik_\perp\cdot b_\perp} \frac{\vec{k}_\perp}{k^2} F_A(k^2) \right|^2$$

Wigner distribution

Wigner distributions [Ji, 03; Belitsky, Ji, Yuan, 2004] encode all quantum information

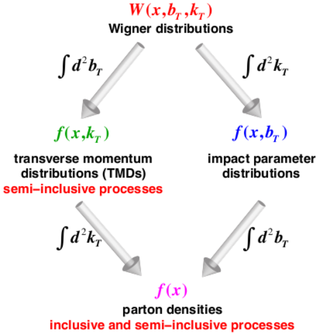

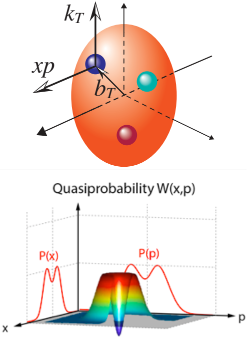

- Quasi-probability distribution; Not positive definite.

Photon Wigner Distribution and Generalized TMD

Def. of Wigner distribution:

$$xf_\gamma(x,\vec{k}_\perp;\vec{b}_\perp) = \int \frac{d\xi^- d^2\xi_\perp}{(2\pi)^3 P^+} \int \frac{d^2\Delta_\perp}{(2\pi)^2} e^{-ixP^+\xi^- - ik_\perp\cdot\xi_\perp}$$
$$\times \quad \left\langle A, +\frac{\Delta_\perp}{2} \middle| F^{+i}\left(\vec{b}_\perp + \frac{\xi}{2}\right) F^{+i}\left(\vec{b}_\perp - \frac{\xi}{2}\right) \middle| A, -\frac{\Delta_\perp}{2} \right\rangle ,$$

Def. of GTMD

$$xf_\gamma(x,k_\perp,\Delta_\perp) \equiv \int d^2b_\perp e^{-i\Delta\cdot b_\perp} xf_\gamma(x,\vec{k}_\perp;\vec{b}_\perp).$$

Photon Wigner Distribution and Generalized TMD

- For a heavy nucleus with charge Ze, the GTMD reads

$$xf_\gamma(x,k_\perp;\Delta_\perp) = xh_\gamma(x,k_\perp;\Delta_\perp) = \frac{4Z^2\alpha}{(2\pi)^2}\frac{q_\perp\cdot q'_\perp}{q^2q'^2}F_A(q^2)F_A(q'^2)\ ,$$

$$q_\perp = k_\perp - \frac{\Delta_\perp}{2}, \quad \text{and} \quad q'_\perp = k_\perp + \frac{\Delta_\perp}{2}$$

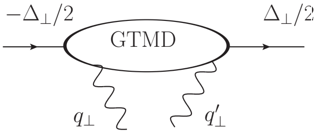

- $\int d^2b_\perp xf_\gamma(x,k_\perp,b_\perp) \Rightarrow TMD$; $\int d^2k_\perp xf_\gamma(x,k_\perp,b_\perp) \Rightarrow b_\perp$ distribution.
- WW EPA $\rightarrow$ Generalized WW EPA with Wigner Photon.

Outline

1 QFT Basics and Theory Backgrounds
- Infrared Safe Observables
- Collinear and TMD Factorization

2 Introduction to Saturation Physics
- Weizsäcker-Williams Methods
- McLerran-Venugopalan Model
- Small-x evolution equations (BFKL + BK)

3 EIC Physics
- Overview
- Observables at EIC

Wilson Lines in Color Glass Condensate Formalism

Wilson line ⇒ multiple scatterings between fast moving quark and target dense gluons.

$$U(x_\perp)=\mathcal{P}\exp\left(-ig\int dz^+A^-(x_\perp,z^+)\right)$$

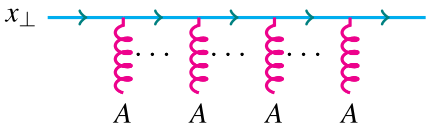

The Wilson loop (color dipole) in McLerran-Venugopalan (MV) model

$$\frac{1}{N_c}\left\langle \mathrm{Tr}U(x_\perp)U^\dagger(y_\perp)\right\rangle=e^{-\frac{Q_s^2(x_\perp-y_\perp)^2}{4}}$$

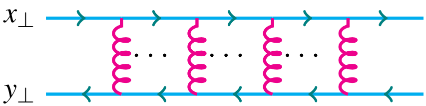

- Dipole amplitude $S^{(2)}$ then produces the quark k_T spectrum via Fourier transform

$$\mathcal{F}(k_\perp)\equiv\frac{dN}{d^2k_\perp}=\int\frac{d^2x_\perp d^2y_\perp}{(2\pi)^2}e^{-ik_\perp\cdot(x_\perp-y_\perp)}\frac{1}{N_c}\left\langle \mathrm{Tr}U(x_\perp)U^\dagger(y_\perp)\right\rangle.$$

A Tale of Two Gluon Distributions[1]

Two gluon distributions are widely used at small-x:[Kharzeev, Kovchegov, Tuchin; 03] I. Weizsäcker Williams gluon distribution([Kovchegov, Mueller, 98] and MV model):

$$xG_{\mathrm{WW}}(x,k_\perp) = \frac{S_\perp}{\pi^2\alpha_s}\frac{N_c^2-1}{N_c}\int\frac{d^2r_\perp}{(2\pi)^2}\frac{e^{-ik_\perp\cdot r_\perp}}{r_\perp^2}\left[1-e^{-\frac{r_\perp^2 Q_{sg}^2}{4}}\right]$$

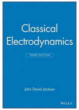

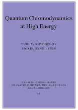

II. Color Dipole gluon distributions: (known for many years)

$$xG_{\mathrm{DP}}(x,k_\perp) = \frac{S_\perp N_c}{2\pi^2\alpha_s}k_\perp^2\int\frac{d^2r_\perp}{(2\pi)^2}e^{-ik_\perp\cdot r_\perp}e^{-\frac{r_\perp^2 Q_{sq}^2}{4}} \Leftarrow \frac{1}{N_c}\mathrm{Tr}\left[U(r_\perp)U^\dagger(0_\perp)\right]$$

[1] As far as I know, the title is due to Y. Kovchegov and C. Dickens.

A Tale of Two Gluon Distributions

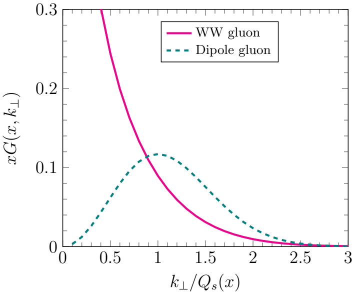

- In McLerran-Venugopalan model, these two gluon distributions exhibit different $k_\perp$ behavior at small $k_\perp$.
- Same tail when $k_\perp \gg Q_s$. "A Tale of Two Gluon Distributions" $\Rightarrow$ "A Tail of Two Gluon Distributions" [B. Zajc]
- Which distribution is measured in a given process?
- Why are there exactly two gluon distributions?

A Tale of Two Gluon Distributions

In terms of operators (TMD def. [Bomhof, Mulders and Pijlman, 06]), two gauge invariant gluon definitions: [Dominguez, Marquet, Xiao and Yuan, 11]

I. Weizsäcker Williams gluon distribution:

$$xG_{\rm WW}(x,k_\perp) = 2\int \frac{d\xi^- d\xi_\perp}{(2\pi)^3 P^+} e^{ixP^+\xi^- - ik_\perp\cdot\xi_\perp} \mathrm{Tr}\langle P|F^{+i}(\xi^-,\xi_\perp)\mathcal{U}^{[+]\dagger}F^{+i}(0)\mathcal{U}^{[+]}|P\rangle.$$

II. Color Dipole gluon distributions:

$$xG_{\rm DP}(x,k_\perp) = 2\int \frac{d\xi^- d\xi_\perp}{(2\pi)^3 P^+} e^{ixP^+\xi^- - ik_\perp\cdot\xi_\perp} \mathrm{Tr}\langle P|F^{+i}(\xi^-,\xi_\perp)\mathcal{U}^{[-]\dagger}F^{+i}(0)\mathcal{U}^{[+]}|P\rangle.$$

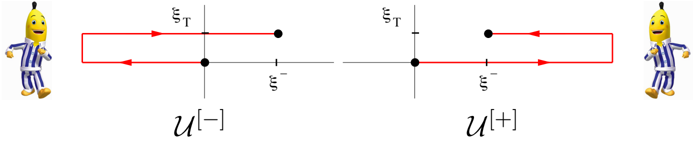

A Tale of Two Gluon Distributions

I. Weizsäcker Williams gluon distribution:

$$xG_{\rm WW}(x,k_\perp) = 2\int \frac{d\xi^- d\xi_\perp}{(2\pi)^3 P^+} e^{ixP^+\xi^- - ik_\perp\cdot\xi_\perp} {\rm Tr}\langle P|F^{+i}(\xi^-,\xi_\perp)\mathcal{U}^{[+]\dagger}F^{+i}(0)\mathcal{U}^{[+]}|P\rangle .$$

II. Color Dipole gluon distributions:

$$xG_{\rm DP}(x,k_\perp) = 2\int \frac{d\xi^- d\xi_\perp}{(2\pi)^3 P^+} e^{ixP^+\xi^- - ik_\perp\cdot\xi_\perp} {\rm Tr}\langle P|F^{+i}(\xi^-,\xi_\perp)\mathcal{U}^{[-]\dagger}F^{+i}(0)\mathcal{U}^{[+]}|P\rangle .$$

- The WW gluon distribution is the conventional gluon distributions.
- The dipole gluon distribution has no such interpretation.
- Two topologically different gauge invariant definitions.
- Same after integrating over $k_\perp$;

A Tale of Two Gluon Distributions

I. Weizs$\ddot{a}$cker Williams gluon distribution

$$xG_{\text{WW}}(x,k_\perp) = \frac{2N_c}{\alpha_S}\int\frac{d^2R_\perp}{(2\pi)^2}\frac{d^2R'_\perp}{(2\pi)^2}e^{iq_\perp\cdot(R_\perp-R'_\perp)} \times\frac{1}{N_c}\left\langle \text{Tr}\left[i\partial_i U(R_\perp)\right]U^\dagger(R'_\perp)\left[i\partial_i U(R'_\perp)\right]U^\dagger(R_\perp)\right\rangle_x$$

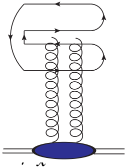

II. Color Dipole gluon distribution:

$$xG_{\text{DP}}(x,k_\perp) = \frac{2N_c}{\alpha_s}\int\frac{d^2R_\perp d^2R'_\perp}{(2\pi)^4}e^{iq_\perp\cdot(R_\perp-R'_\perp)} \left(\nabla_{R_\perp}\cdot\nabla_{R'_\perp}\right)\frac{1}{N_c}\left\langle\text{Tr}\left[U(R_\perp)U^\dagger(R'_\perp)\right]\right\rangle_x ,$$

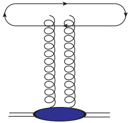

- Quadrupole $\Rightarrow$ Weizs$\ddot{a}$cker Williams gluon distribution;
- Dipole $\Rightarrow$ Color Dipole gluon distribution;

A Tale of Two Gluon Distributions

Measuring the gluon distributions in various processes

I. Weizsäcker Williams gluon distribution; II. Color Dipole gluon distributions.

- Modified Universality for Gluon Distributions:

	Inclusive	Single Inc	DIS dijet	γ +jet	dijet in pA
xG_{WW}	$\times$	$\times$	$\surd$	$\times$	$\surd$
xG_{DP}	$\surd$	$\surd$	$\times$	$\surd$	$\surd$

$\times \Rightarrow$ Do Not Appear. $\surd \Rightarrow$ Apppear.

- Measurements in pA collisions and at the EIC are tightly connected with complementary physics missions.
- At higher order, Sudakov resummation needs to be implemented, but the conclusion remains true. Soft gluon factorizes. [Mueller, Xiao, Yuan, 13]

Outline

1 QFT Basics and Theory Backgrounds
- Infrared Safe Observables
- Collinear and TMD Factorization

2 Introduction to Saturation Physics
- Weizsäcker-Williams Methods
- McLerran-Venugopalan Model
- Small-x evolution equations (BFKL + BK)

3 EIC Physics
- Overview
- Observables at EIC

Deep into low-x region of Protons

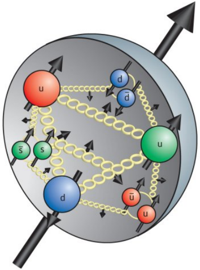

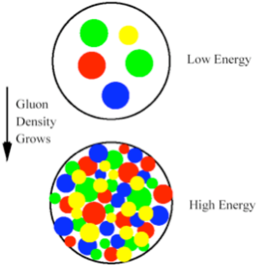

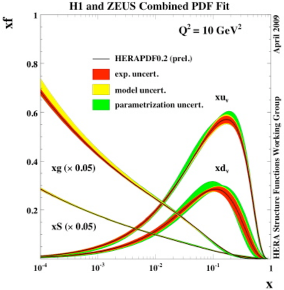

- Gluon splitting functions ($\mathcal{P}^0_{qq}(\xi)$ and $\mathcal{P}^0_{gg}(\xi)$) have $1/(1-\xi)$ singularities.
- Partons in the low-x region is dominated by gluons.
- Resummation of the $\alpha_s \ln \frac{1}{x}$.

Dual Descriptions of Deep Inelastic Scattering

[A. Mueller, 01; Parton Saturation-An Overview]

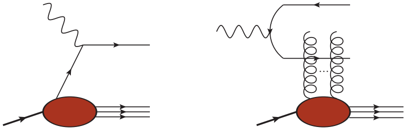

Bjorken frame Dipole frame

Bjorken frame

$$F_2(x,Q^2) = \sum_q e_q^2 x \left[f_q(x,Q^2) + f_{\bar{q}}(x,Q^2) \right] .$$

- Bjorken: partonic picture of a hadron is manifest. Saturation shows up as a limit on the occupation number of quarks and gluons.

Dual Descriptions of Deep Inelastic Scattering

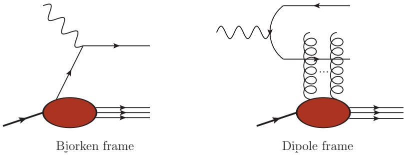

Dipole frame

$$F_2(x,Q^2) = \sum_f e_f^2 \frac{Q^2}{4\pi^2\alpha_{\rm em}} \int_0^1 \mathrm{d}z \int \mathrm{d}^2x_\perp \mathrm{d}^2y_\perp \left[|\psi_T(z,r_\perp,Q)|^2 + |\psi_L(z,r_\perp,Q)|^2\right] \times [1 - S(r_\perp)], \quad \text{with} \quad r_\perp = x_\perp - y_\perp .$$

- Dipole: partonic picture is no longer manifest. Saturation appears as the unitarity limit for scattering. Easy to resum the multiple gluon interactions.
- Interesting property: Geometric scaling if $S(r_\perp) = S(Q_s r_\perp)$.

BFKL evolution

[Balitsky, Fadin, Kuraev, Lipatov;74] Bremsstrahlung favors of small-x gluon emissions.

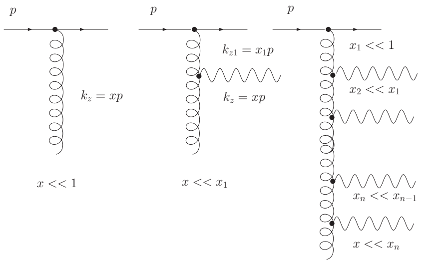

Probability of emission:

$$dp \sim \alpha_s N_c \frac{dk_z}{k_z} = \alpha_s N_c \frac{dx}{x}$$

In small-x limit and Leading log approximation:

$$p \sim \sum_{n=0}^{\infty} \alpha_s^n N_c^n \int_x^1 \frac{dx_n}{x_n} \cdots \int_{x_2}^1 \frac{dx_1}{x_1} \sim \exp\left(\alpha_s N_c \ln \frac{1}{x}\right)$$

- Cf. DGLAP which resums $\alpha_s C \ln \frac{Q^2}{\mu_0^2}$.

Exponential growth of the amplitude as function of rapidity;

Derivation of BFKL evolution

[Mueller, 94] Dipole model: Consider the emission of soft gluon $z_g \ll 1$,

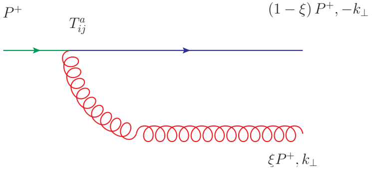

and use LC gauge $\epsilon = (\epsilon^+ = 0, \epsilon^- = \frac{\epsilon_\perp \cdot k_\perp}{k^+}, \epsilon_\perp^\pm)$

$$\mathcal{M}(k_\perp) = -2igT^a \frac{\epsilon_\perp \cdot k_\perp}{k_\perp^2}$$

- $q \to qg$ vertex and Energy denominator.
- Similar to the derivation of $\mathcal{P}_{qq}(\xi)$.

The dipole splitting kernel

The Bremsstrahlung amplitude in the coordinate space

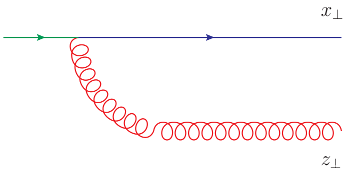

$$\mathcal{M}(x_\perp - z_\perp) = \int d^2k_\perp e^{ik_\perp\cdot(x_\perp - z_\perp)}\mathcal{M}(k_\perp)$$

$$\text{Use} \quad \int d^2k_\perp \frac{\epsilon_\perp \cdot k_\perp}{k_\perp^2} e^{ik_\perp\cdot b_\perp} = 2\pi i \frac{\epsilon_\perp \cdot b_\perp}{b_\perp^2},$$

$$\Rightarrow \quad \mathcal{M}(x_\perp - z_\perp) = 4\pi g T^a \frac{\epsilon_\perp \cdot (x_\perp - z_\perp)}{(x_\perp - z_\perp)^2}$$

The dipole splitting kernel

Consider soft gluon emission from a color dipole in the coordinate space $(x_\perp, y_\perp)$

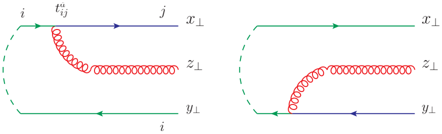

$$\mathcal{M}(x_\perp, z_\perp, y_\perp) = 4\pi g T^a \left[\frac{\epsilon_\perp \cdot (x_\perp - z_\perp)}{(x_\perp - z_\perp)^2} - \frac{\epsilon_\perp \cdot (y_\perp - z_\perp)}{(y_\perp - z_\perp)^2} \right] \Rightarrow$$

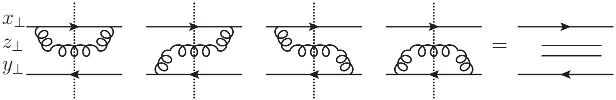

$$= \frac{\alpha_s N_c}{2\pi^2} \frac{(x_\perp - y_\perp)^2}{(x_\perp - z_\perp)^2 (y_\perp - z_\perp)^2}$$

The dipole splitting kernel

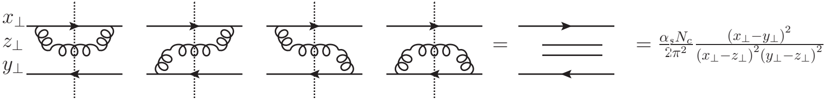

- The probability of dipole splitting at large N_c limit

$$dP_{\text{splitting}} = \frac{\alpha_s N_c}{2\pi^2} \frac{(x_\perp - y_\perp)^2}{(x_\perp - z_\perp)^2 (x_\perp - z_\perp)^2} \mathrm{d}^2 z_\perp \mathrm{d}Y \quad \text{with} \quad \mathrm{d}Y = \frac{\mathrm{d}k_g^+}{k_g^+}$$

- Gluon splitting $\Leftrightarrow$ Dipole splitting.

BFKL evolution in Mueller's dipole model

[Mueller; 94] In large N_c limit, BFKL evolution can be viewed as dipole branching in a fast moving $q\bar{q}$ dipole in coordinate space:

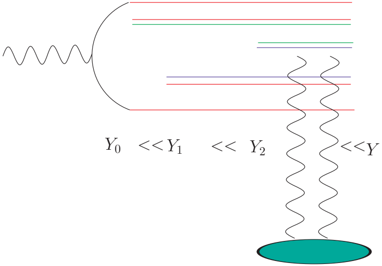

$n(r, Y)$ dipoles of size r.

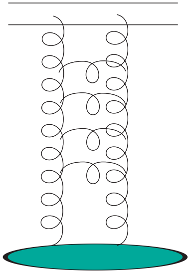

BFKL Pomeron

The T matrix ($T \equiv 1 - S$ with S being the scattering matrix) basically just counts the number of dipoles of a given size,

$$T(r, Y) \sim \alpha_s^2 n(r, Y)$$

BFKL equation

Consider a slight change in rapidity and the Bremsstrahlung emission of soft gluon (dipole splitting)

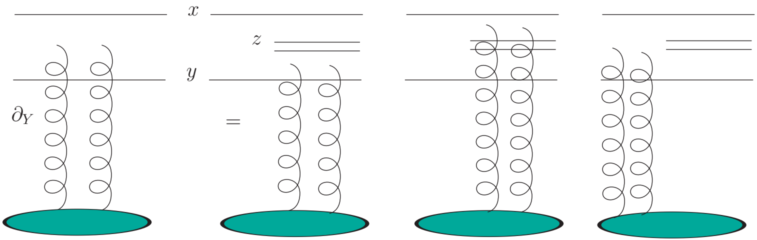

$$\partial_Y T(x,y;Y) = \frac{\bar{\alpha}_s}{2\pi}\int d^2z \frac{(x-y)^2}{(x-z)^2(z-y)^2}\left[T(x,z;Y)+T(z,y;Y)-T(x,y;Y)\right]$$

Kovchegov equation

[Kovchegov; 99] [Mueller; 01] Including non-linear effects: ($T \equiv 1 - S$)

$\frac{\partial S}{\partial Y} =$ 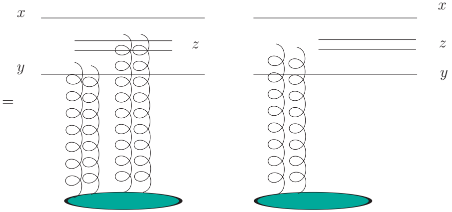

$$\partial_Y S(x-y;Y) \quad = \quad \frac{\alpha N_c}{2\pi^2}\int d^2z \frac{(x-y)^2}{(x-z)^2(z-y)^2}\left[S(x-z;Y)S(z-y;Y) - S(x-y;Y)\right]$$

- Linear BFKL evolution results in fast energy evolution.
- Allowing multiple scattering $\Rightarrow$ Non-linear term

Kovchegov equation

[Kovchegov; 99] [Mueller; 01] Including non-linear effects: $(T \equiv 1 - S)$

$$\partial_Y S(x-y;Y) = \frac{\alpha N_c}{2\pi^2}\int d^2z \frac{(x-y)^2}{(x-z)^2(z-y)^2}\left[S(x-z;Y)S(z-y;Y) - S(x-y;Y)\right]$$

$$\partial_Y T(x-y;Y) = \frac{\alpha N_c}{2\pi^2}\int d^2z \frac{(x-y)^2}{(x-z)^2(z-y)^2} \times \left[T(x-z;Y) + T(z-y;Y) - T(x-y;Y) - \underbrace{T(x-z;Y)T(z-y;Y)}_{saturation}\right]$$

- Linear BFKL evolution results in fast energy evolution $\Rightarrow$ saturation region
- Non-linear term $\Rightarrow$ fixed point $(T = 1)$ and unitarization, and thus describes the saturation physics.

Balitsky-Kovchegov equation vs F-KPP equation

[Munier, Peschanski, 03] Consider the case with fixed impact parameter, namely, T_{xy} is only function of $r = x - y$. Then, transforming the B-K equation into momentum space:

BK equation: $\partial_Y T = \bar{\alpha}\chi_{\text{BFKL}}(-\partial_\rho)T - \bar{\alpha}T^2$ with $\bar{\alpha} = \frac{\alpha N_c}{\pi}$

Diffusion approximation $\Rightarrow$

F-KPP equation: $\partial_t u(x,t) = \partial_x^2 u(x,t) + u(x,t) - u^2(x,t)$

- $u \Rightarrow T$, $\bar{\alpha}Y \Rightarrow t$, $\varrho = \log(k^2/k_0^2) \Rightarrow x$, with k_0 being the reference scale;
- B-K equation lies in the same universality class as the F-KPP [Fisher-Kolmogrov-Petrovsky-Piscounov; 1937] equation.
- F-KPP eq admits traveling wave solution $u = u\,(x - vt)$ with minimum velocity
- The non-linear term saturates the solution in the infrared.

Outline

1 QFT Basics and Theory Backgrounds
- Infrared Safe Observables
- Collinear and TMD Factorization

2 Introduction to Saturation Physics
- Weizsäcker-Williams Methods
- McLerran-Venugopalan Model
- Small-x evolution equations (BFKL + BK)

3 EIC Physics
- Overview
- Observables at EIC

HERA (Hadron Elektron Ring Anlage)

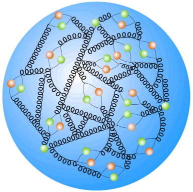

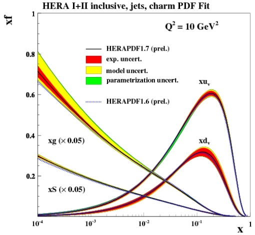

- $e^{\pm}p$ collisions at $\sqrt{s} = 318\,\text{GeV}$ (1992-2007);
  - Partons in the low-x region is dominated by rapid growing gluons.

Geometrical Scaling in DIS

[Golec-Biernat, Stasto, Kwiecinski; 01, Munier, Peschanski, 03]

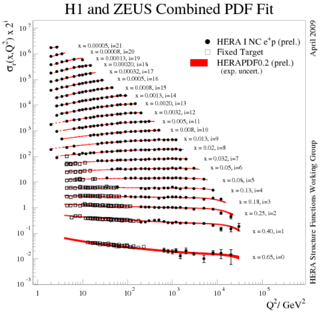

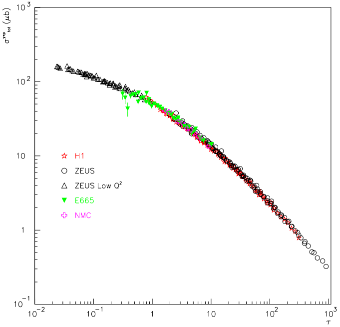

- Use $Q_s^2(x) = (x_0/x)^\lambda \mathrm{GeV}^2$ with $x_0 = 3.04 \times 10^{-3}$ and $\lambda = 0.288$. All data of $\sigma_{tot}^{\gamma^* p}$ with $x \leq 0.01$ and $Q^2 \leq 450 GeV^2$ plotting as function of a single variable $\tau = Q^2/Q_s^2$.
- This scaling can be naturally explained in small-x formalism.

Ultimate Questions and Challenges in QCD

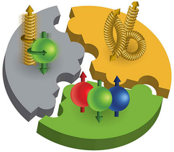

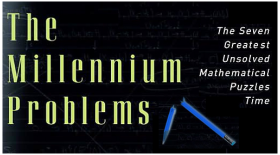

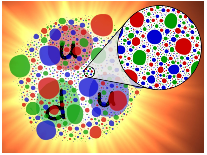

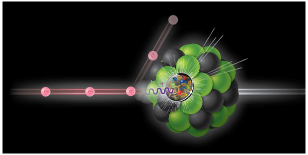

- How does the spin of proton arise? (Spin puzzle)
- What are the emergent properties of dense gluon system?
- How does proton mass arise? Mass gap: million dollar question.
- How does gluon bind quarks and gluons inside proton?
- Can we map the quark and gluon inside the proton in 3D?

EICs: keys to unlocking these mysteries! Many opportunities will be in front of us!

Embedding small-x gluon in 3D Tomography

Wigner distributions [Belitsky, Ji, Yuan, 04] ingeniously encode all quantum information of how partons are distributed inside hadrons.

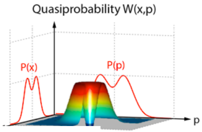

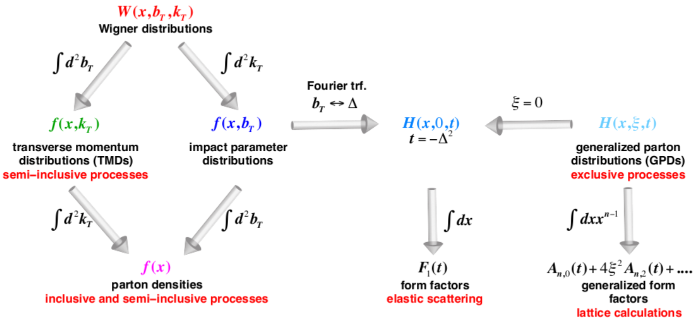

List of observables at EIC

- CGC is elusive.
- Hunt it down via a set of observables
- List it from Inclusive $\rightarrow$ Exclusive.

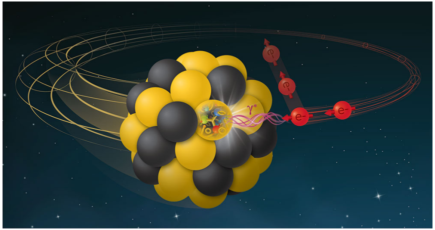

1. Inclusive cross-section: Geometrical scaling in eA and Q_{sA}
2. Single-inclusive $\gamma + p/A \rightarrow h(\text{Jet}) + X$: Quark TMD
3. Inclusive dijet or dihadron: WW gluon TMD.
4. Long range correlation: Origin of collectivity
5. Diffractive vector meson production: gluon GPD.
6. Diffractive dijet production: gluon Wigner distribution.

Outline

1 QFT Basics and Theory Backgrounds
- Infrared Safe Observables
- Collinear and TMD Factorization

2 Introduction to Saturation Physics
- Weizsäcker-Williams Methods
- McLerran-Venugopalan Model
- Small-x evolution equations (BFKL + BK)

3 EIC Physics
- Overview
- Observables at EIC

Inclusive Observables

- Geometrical Scaling in DIS: All data of $\sigma_{tot}^{\gamma^* p}$ with $x \leq 0.01$ and $Q^2 \leq 450 GeV^2$ plotting as function of a single variable $\tau = Q^2/Q_s^2$ falls on a curve.
- What about eA collisions at EIC? $Q_{sA}^2(x)$

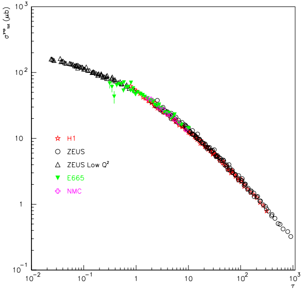

- [Golec-Biernat, Stasto, Kwiecinski,01]: $Q_s^2(x) = (x_0/x)^\lambda \mathrm{GeV}^2$ with $x_0 = 3.04 \times 10^{-3}$ and $\lambda = 0.288$.
- [Munier, Peschanski, 03]: explained by traveling wave in small-x framework.
- [Kovchegov, Pitonyak, Sievert, 16, 17] Link Polarized case: g_1 structure function at small-x and $\Delta\Sigma$.

SIDIS and new progress

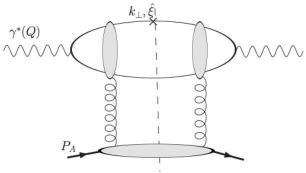

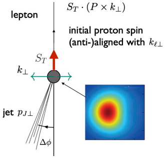

Electron-jet corretions

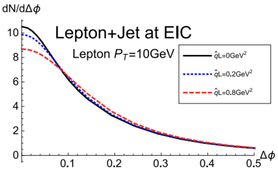

- [Mueller, 99; Marquet, Xiao, Yuan, 09] SIDIS in Breit frame: $\Rightarrow$ quark k_T TMD.
- [Liu, Ringer, Vogelsang, Yuan,19] Link Lepton + jet

New hard probe in the Lab frame: $\quad l + p/A \to l' + \text{Jet} + X$

- Direct probe of quark TMDs. $\Delta\phi = \phi_J - \phi_l - \pi$
- Sivers: distortion due to proton's transverse spin S_T!
- Also sensitive to cold nuclear medium P_T broadening!

Leton-jet correlations at EIC

[Hatta, Xiao, Yuan, Zhou, 21] ▸ 2106.05307 [hep-ph]

$$e(k)+q(p_1)\to e'(k_\ell)+jet(k_J)+X$$

$$g^2\int\frac{d^3k_g}{(2\pi)^3 2E_{k_g}}\delta^{(2)}(q_\perp+k_{g\perp})C_F S_g(k_J,p_1)$$
$$=\frac{\alpha_s C_F}{2\pi^2 q_\perp^2}\left[\ln\frac{Q^2}{q_\perp^2}+\ln\frac{Q^2}{k_{\ell\perp}^2}\right.$$
$$\left.+c_0+2c_1\cos(\phi)+2c_2\cos(2\phi)+\cdots\right],$$

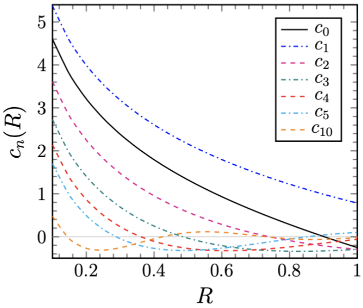

- Asymmetric emission of gluons outside jet cone.
- Eikonal factors $S_g(k_J,p_1)=\frac{2k_J\cdot p_1}{k_J\cdot k_g p_1\cdot k_g}$; $S_g(k_1,k_2)=\frac{2k_1\cdot k_2}{k_1\cdot k_g k_2\cdot k_g}$. ▸ QCD Master Class 2021

DIS dijet

Unique golden channel for the Weizsäcker Williams distribution.

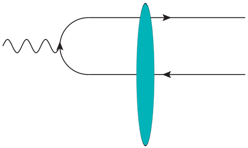

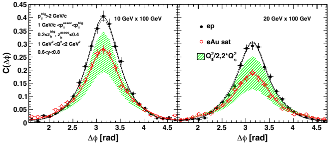

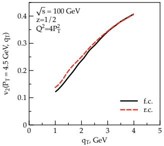

- Back-to-back correlation $C(\Delta\phi)$: [Dominguez, Marquet, Xiao and Yuan, 11] [Zheng, Aschenauer, Lee and BX, 14] Link
- Due to soft gluon radiations, Sudakov resummation needs to be implemented. [Mueller, Xiao, Yuan, 13] Link
- Due to linearly polarized gluon[Metz, Zhou, 11] Link: analog of elliptic flow v_2 in DIS. [Dumitru, Lappi, Skokov, 15] Link

Perturbative expansions in dijet productions

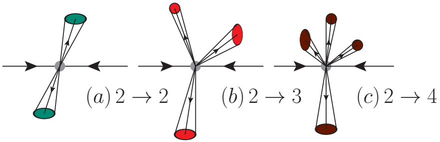

Correlations:

$2 \to 2$: 0th order
$2 \to 3$: leading order
$2 \to 4$: next-to-leading order

$\sigma_0 \sum_{i=0}^{\infty} \alpha_s^i \left(L^i + C^{(i)} \right)$ ideal QCD expansion

$\sigma_0 \sum_{i=0}^{n-1} \alpha_s^i L^i$	$\sigma_0 \sum_{i=0}^{n-1} \alpha_s^i C^{(i)}$	$\Leftarrow$ pQCD
$\sigma_0 \sum_{i=n}^{\infty} \alpha_s^i L^i$	$\sigma_0 \sum_{i=n}^{\infty} \alpha_s^i C^{(i)}$	$\nwarrow$ negligible
$\Uparrow$ resummation		

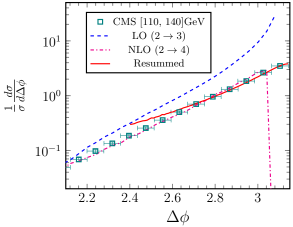

- Appearance of large logarithms $L \sim \ln^2 \frac{P_\perp^2}{q_\perp^2}$ (pQCD expansion breaks down)
- Imbalance $\vec{q}_\perp \equiv \vec{p}_{1\perp} + \vec{p}_{2\perp}$, jet $P_\perp \sim p_{1\perp} \sim p_{2\perp}$.

Sudakov formalism

Dijet productions in the Sudakov formalism (starting from collinear factorization)

$$\begin{aligned}
\frac{d\sigma_{\text{dijet}}}{dy_1 dy_2 d^2p_{1\perp} d^2p_{2\perp}} &= \sum_{ab} \sigma_0 \int \frac{d^2b_\perp}{(2\pi)^2} e^{-iq_\perp \cdot b_\perp} W(Q, b_\perp), \\
\text{with} \quad W(Q, b_\perp) &= x_1 f_a(x_1, \mu_b) x_2 f_b(x_2, \mu_b) e^{-S(Q, b_\perp)}, \\
S(Q, b_\perp) &= S_{pert}(Q, b_*) + S_{NP}(Q, b_\perp) \\
S_{pert}(Q, b_*) &= \int_{\mu_b^2 = c_0^2/b_*^2}^{Q^2} \frac{d\mu^2}{\mu^2} \left[A \ln \frac{Q^2}{\mu^2} + B + (D_1 + D_2) \ln \frac{1}{R^2} \right].
\end{aligned}$$

Sudakov formalism

- Soft gluon emissions factorize from the born cross section σ_0.
- Resummation is performed in the $b_\perp$ space. Use $\delta^{(2)}(k_\perp - q_\perp) = \int \frac{d^2b_\perp}{(2\pi)^2} e^{i(k_\perp - q_\perp)\cdot b_\perp}$

$$\begin{aligned}\frac{d\sigma}{d^2q_\perp} &= \sigma_0 \sum_n \frac{(-1)^n}{n!} \int d^2k_{1\perp} \cdots d^2k_{n\perp} S(k_{1\perp}) \cdots S(k_{n\perp}) \delta^{(2)}(k_{1\perp} + \cdots k_{n\perp} - q_\perp) \\ &= \sigma_0 \int \frac{d^2b_\perp}{(2\pi)^2} e^{-iq_\perp \cdot b_\perp} e^{-S(b_\perp)}\end{aligned}$$

- Use $b_* = b/\sqrt{1 + b^2/b_{max}^2}$ prescription to separate perturbative and NP regions.
- All the A, B, C, D coefficients can be computed perturbatively.

QCD Sudakov (CSS) Resummation for Boson Productions

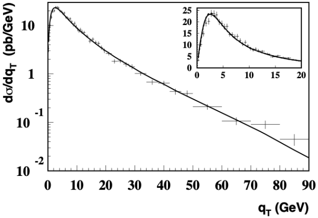

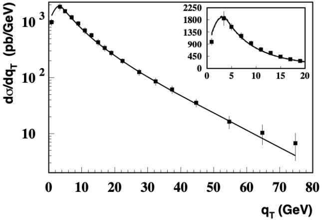

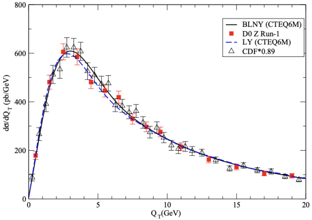

[J.w. Qiu and X. Zhang, 02] DY and *W*   [Landry, Brok, Nadolsky, C. Yuan, 03] *Z* boson

Collectivity at EIC?

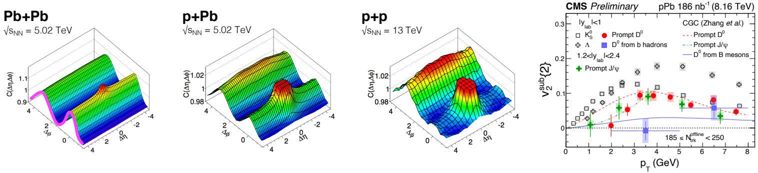

- Collectivity is everywhere in systems small and large!
- Final state vs Initial state interpretation. Not clear yet!
- Anisotropy of heavy mesons favors IS effect.
  [Zhang, Marquet, Qin, Wei, Xiao, 19] ▸ Link
- New results from UPC in PbPb collisions at LHC. (Mini-EIC)
- What about the collectivity at the EIC on the horizon?

v_2 Predictions in γA collisions from CGC

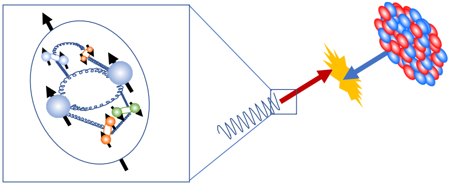

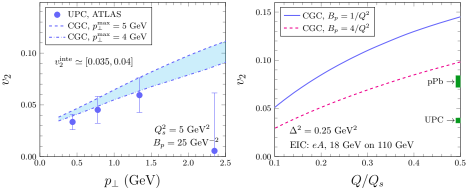

[Shi, Wang, Wei, Xiao, Zheng, 21] Link

- Photons can have a rich QCD structure due to fluctuation.
- Similarity between $\gamma^* A$ and pA collisions at high energy as far as high multiplicity events are concerned.

Explicit expressions for gluon GPDs

Small-x GPDs[Hatta, Xiao, Yuan, 17] Link $F = F_0 + 2\cos 2\Delta\phi\, F_\epsilon$

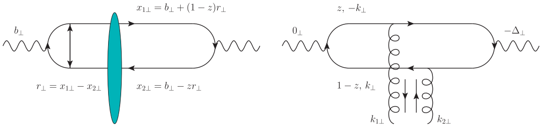

$$\frac{1}{P^+}\int \frac{d\zeta^-}{2\pi} e^{ixP^+\zeta^-} \langle p'|F^{+i}(-\zeta/2)F^{+j}(\zeta/2)|p\rangle$$
$$= \frac{\delta^{ij}}{2} xH_g(x,\Delta_\perp) + \frac{xE_{Tg}(x,\Delta_\perp)}{2M^2}\left(\Delta_\perp^i\Delta_\perp^j - \frac{\delta^{ij}\Delta_\perp^2}{2}\right) + \cdots,$$

Helicity conserved: $xH_g(x,\Delta_\perp) = \frac{2N_c}{\alpha_s}\int d^2q_\perp q_\perp^2 F_0$

Helicity flipping: $xE_{Tg}(x,\Delta_\perp) = \frac{4N_cM^2}{\alpha_s\Delta_\perp^2}\int d^2q_\perp q_\perp^2 F_\epsilon$

Gluon GPDs and DVMP $V = J/\Psi, \phi \cdots$

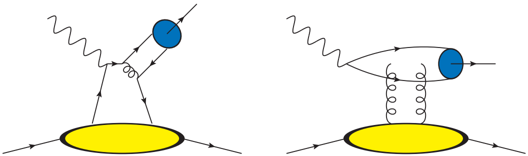

$$\gamma^*(q) + p/A(p) \to V(q - \Delta) + p/A(p + \Delta)$$

- The latter diagram is dominant at small-x (high energy) limit.
- Widely studied[Brodsky, Frankfurt, Gunion, Mueller, Strikman, 94; Kowalski, Teaney, 03; Kowalski, Motyka, Watt, 06; Kowalski, Caldwell, 10; Berger, Stasto, 13; Rezaeian, Schmidt, 13]...
- Incoherent diffractive production for nucleon/nuclear targets [T. Lappi, H. Mantysaari, 11; Toll, Ullrich, 12; Lappi, Mantysaari, R. Venugopalan, 15; Lappi, Mantysaari, Schenke, 16]...;
- NLO[Boussarie, Grabovsky, Ivanov, Szymanowski, Wallon, 16] Link

Probing gluon GPD at small-x

DVCS and DVMP [Mantysaari, Roy, Salazar, Schenke, 20] Link

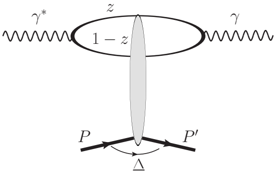

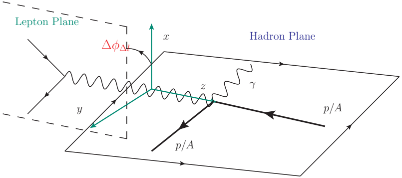

$$\frac{d\sigma_{TT}}{dx_B dQ^2 d^2\Delta_\perp} = \frac{\alpha_{em}^3}{\pi x_{Bj} Q^2}\left\{\left(1-y+\frac{y^2}{2}\right)(\mathcal{A}_0^2+\mathcal{A}_2^2)+(1-y)2\mathcal{A}_0\mathcal{A}_2\cos(2\phi_{\Delta l})\right\}$$

- $\mathcal{A}_0$: helicity conserved amplitude; $\mathcal{A}_2$: helicity-flip amplitude
- Use lepton plane as reference, one can measure angular correlations.
- $\cos 2\phi_{\Delta l}$ correlation is sensitive to the helicity-flip gluon GPD xE_{Tg}.

Diffractive vector meson production

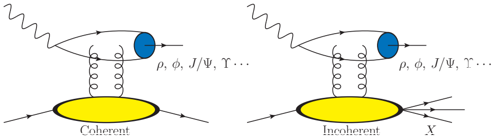

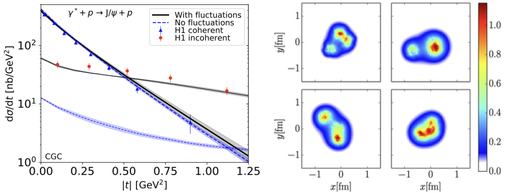

- Sensitive to proton fluctuating shape. (Variance) [Mantysaari, Schenke, 16; Mantysaari, Roy, Salazar, Schenke, 20]
- Good-Walker: measure of fluct. $\frac{d\sigma_{\text{incoh}}}{d\hat{t}} \sim \langle |\mathcal{A}|^2 \rangle - |\langle \mathcal{A} \rangle|^2$

Can we measure Wigner distributions?

- Can we measure Wigner distribution/GTMD? Yes, we can!
- Diffractive back-to-back dijets in *ep*/*eA* collisions. [Hatta, Xiao, Yuan, 16] Link
- Further predictions of asymmetries due to correlations.

$$
\begin{aligned}
xW_g^T(x,\vec{q}_\perp;\vec{b}_\perp) &= x\mathcal{W}_g^T \quad \text{Symmetric part} \\
&+ 2\cos(2\phi)x\mathcal{W}_g^\epsilon + \cdots \quad \text{Anisotropies}
\end{aligned}
$$

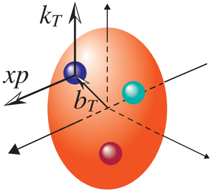

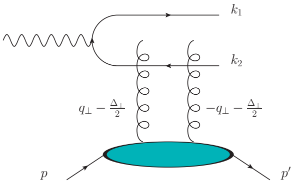

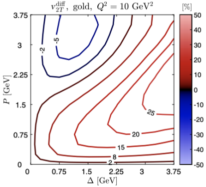

- Study of the elliptic anisotropy.[Mäntysaari, Mueller, Salazar and Schenke, 20] Link

CMS: Dijet photoproduction in UPC (PbPb)

$$\gamma + \text{Pb} \to \text{Jet} + \text{Jet} + \text{Pb}$$

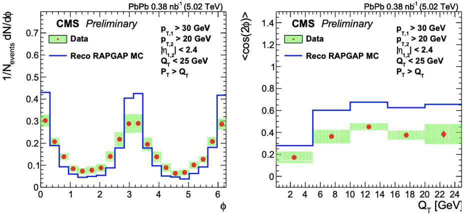

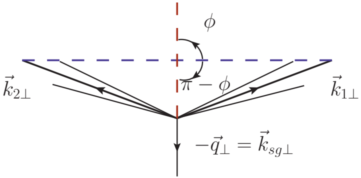

1. Preliminary analysis ▸ Link [CMS-PAS-HIN-18-011]
2. Large asymmetries observed!
3. Indicate additional sources ?

Asymmtries due to final state gluon radiations are important.
[Hatta, Xiao, Yuan, Zhou, 21] ▸ Link

Contributions from final state gluon radiations

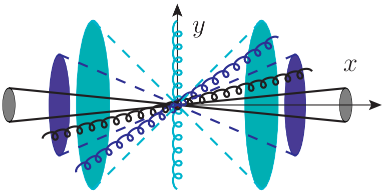

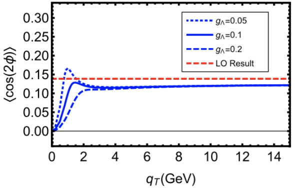

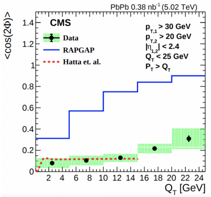

Consider soft gluon radiations near jet cone in $\gamma A/p \to q\bar{q} + A/p$

$$g^2 \int \frac{d^3k_g}{(2\pi)^3 2E_{k_g}} \delta^{(2)}(q_\perp + k_{g\perp}) C_F \frac{2k_1 \cdot k_2}{k_1 \cdot k_g k_2 \cdot k_g}$$

$$= \frac{C_F \alpha_s}{\pi^2 q_\perp^2} \left[c_0^{\text{diff}} + 2\cos(2\phi)\, c_2^{\text{diff}} + \ldots\right].$$

$$c_0^{\text{diff}} = \ln \frac{a_0}{R^2}, \qquad c_2^{\text{diff}} = \ln \frac{a_2}{R^2}.$$

Observed asymmetry should includes initial and final state contributions!

Summary of the Lectures

- Lecture 1 - Introduction to QCD and Jet
  - Infrared Safe Observable
  - Collinear Factorization and DGLAP equation
- Lecture 2 - Saturation Physics (Color Glass Condensate)
  - McLerran-Venugopalan Model
  - BFKL equation
  - Non-linear small-x evolution equations
- Lecture 3 - EIC observables